Progress in Natural Science: Materials International 2013;23(2):205–210

Chinese Materials Research Society

Progress in Natural Science: Materials International

www.elsevier.com/locate/pnsmi
www.sciencedirect.com

ORIGINAL RESEARCH

Effects of temperature and stress on the creep behavior of a Ni_3Al base single crystal alloy

Zhigang Kong[a], **Shusuo Li**[b,*]

[a]*School of Automation, Beijing University of Post and Telecommunications, 10 Xitucheng Road, Haidian District, Beijing 100876, China*
[b]*School of Materials Science and Engineering, Beihang University, Beijing 100083, China*

Received 8 November 2012; accepted 5 January 2013
Available online 24 April 2013

KEYWORDS

Single crystal;
Ni_3Al alloy;
Creep;
Dislocation

Abstract The creep behavior and microstructure of a Ni_3Al base single crystal alloy IC6SX with [001] orientation under the testing conditions of 760 °C/593 MPa, 980 °C/205 MPa, and 1100 °C/75 MPa were investigated. The experimental results showed that Alloy IC6SX had good creep resistance and its creep resistance at elevated temperatures was similar to the second generation nickel-base single crystal alloy containing Re. TEM analysis indicated that the dislocation configuration and movement pattern were different under different temperature and stress conditions. It has been found that under the test condition of 1070 °C/137 MPa the dislocations moved within the γ channel during the primary creep stage, and the motion of dislocations were prevented by the matrix of γ′ phase, which reduced the creep rate of the alloy. In the secondary creep stage, dislocations cut into the γ′ phase from the γ/γ′ interface. However in the third creep stage, the dislocation pileups were observed in both γ and γ′ phase, and dislocation multiplication occurred when the dislocations with different Burgers vector met and reacted each other.

1. Introduction

The evolution of efficient gas turbine engine technology has brought about increased interest in high temperature creep resistant materials for the usage of turbine blades and vanes [1–6]. The nickel base single crystal superalloy is the most important material for advanced turbine blades. In order to increase the high temperature creep resistance, the very expensive element rhenium (Re) is added in the second (containing 3% Re) and third (containing 5–6% Re) generation nickel base single crystal superalloys, respectively. Since the addition of high amount Re in alloys

*Corresponding author. Tel.: +86 10 62283173.
E-mail addresses: zgkong@bupt.edu.cn (Z. Kong), lishs@buaa.edu.cn (S. Li).

Peer review under responsibility of Chinese Materials Research Society.

Production and hosting by Elsevier

1002-0071 © 2013 Chinese Materials Research Society. Production and hosting by Elsevier B.V. All rights reserved.
http://dx.doi.org/10.1016/j.pnsc.2013.03.005

make the second and third generation nickel base single crystal superalloys very expensive, and the Re resource in the earth is very limited, the development of low cost superalloy without Re is necessary for the materials scientists. A directionally solidified Ni_3Al-base alloy IC6 without expensive elements was developed used for advanced jet-engine blades and vanes operating in the temperature range of 1050–1150 °C [7,8]. The alloy IC6 has some merits, such as low density (7.9 g/cm^3), low cost, high melting temperature (1315 °C) and high mechanical properties. Alloy IC6 has being successfully used for turbine vanes of aero-engines [9,10]. In order to further improve the high temperature creep resistance meeting the requirement of turbine blade material with the operating temperatures up to 1100 °C, the Ni_3Al base single crystal alloy named as IC6SX has been recently developed based on the DS alloy IC6. Alloy IC6SX has excellent creep resistance compared with commercial second generation Ni base single crystal superalloys. The effects of element content, microstructure, and the withdrawal rate on stress rupture and creep properties on Ni_3Al-base alloy was studied earlier [11–13]. Hemker studied the intermediate temperature creep of Ni_3Al, and found that primary octahedral glide, the dislocation mechanism responsible for the yield strength anomaly, is exhausted by the formation of Kear–Wilsdorf locks during primary creep [14].

In this paper, the effect of temperature and stress level on the creep behavior and creep mechanisms of the Ni_3Al base single crystal alloy IC6SX have been investigated.

2. Experimental procedure

The material used for the present study was a Ni_3Al base alloy IC6SX, with a nominal composition of Ni-7.6Al–14Mo (wt%). The single crystal samples were produced by screw selection crystal method with the drawing rate of 4 mm/min, and then heat treated under the condition of 1300 °C/10 h+870 °C/32 h. The creep specimens with the gauge length of 27 ± 0.1 mm and the diameter of 5.00 ± 0.02 mm were cut from the heat-treated samples. The creep tests were carried out in air by constant load creep machines under the conditions of 760 °C/593 Mpa, 980 °C/205 Mpa, 1070 °C/137 MPa and 1100 °C/75 MPa, respectively. The testing temperature and the fluctuations along the gauge length were controlled within ± 1 °C during the testing. The disk samples for microstructure observation were cut from the gauge length part of the creep specimens deformed under the above three different conditions. The morphology and composition of the creep tested specimens were examined by JSM-5800 scanning electron microscope (SEM) and Link ISIS 6498 energy dispersive spectroscopy (EDS). The dislocation configuration of the crept specimens was observed by JEM-2100F transmission electron microscope (TEM).

Table 1 Tensile stress rupture lives of IC6SX alloy under 1100 °C/130 MPa.

Specimen No.	Orientation	Dev. degree (deg)	Life (h)
I	<001>	8	58:05, 80:00
II	<011>	18	88:00, 67:00
III	<111>	15	239:35, 108:30

3. Results and discussion

3.1. Creep behavior of the alloy

The stress rupture lives of the alloy with different orientation under the testing conditions of 1100 °C/130 MPa are listed in Table 1. The results show that the specimens have good stress rupture

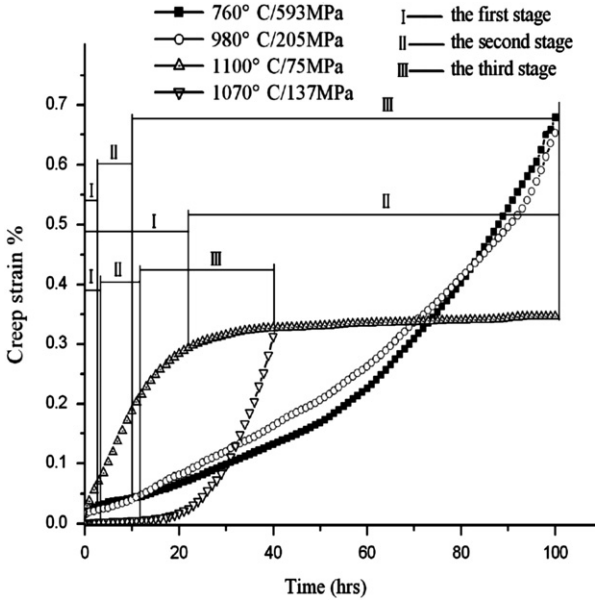

Fig. 1 Creep curves of the alloy under different test conditions.

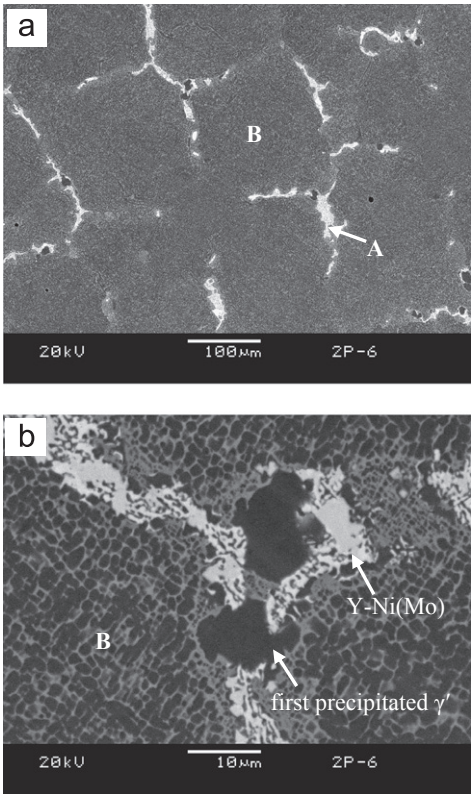

Fig. 2 Back scattered electron image (BSEI) of as-cast IC6SX alloy.

property, which are similar to the stress rupture lives of the second generation nickel base single crystal superalloys (containing 3% Re).

The creep testing and analysis was performed on Ni_3Al specimens with a tensile axis orientation deviated 7–9° from [001] orientation. The creep curves of the alloys under the testing conditions of 760 °C/593 MPa, 980 °C/205 MPa, 1070 °C/137 MPa and 1100 °C/75 MPa are shown in Fig. 1. It can be seen that, for the curves of 760 °C/593 MPa and 980 °C/205 MPa, the first and second stages of creep process are short, and the third stage was observed after 10 h creep test. After 100 h creep test, the creep strain reached to about 0.6–0.7%. However, the creep curves of 1100 °C/75 MPa show that the first creep stage time lasted for about 20 h and the second stage lasted until the end of the 100 h test. Different from the curves of 760 °C/593 MPa and 980 °C/205 MPa, the third stage was not observed. It has been found that in the secondary creep stage, the strain rate is about 0.35%, which is obviously lower than those under 760 °C/593 MPa, 980 °C/205 MPa. The results indicate that the alloy has long time and good creep properties under the test condition of 1100 °C/75 MPa. The creep curve of the specimen under 1070 °C/137 MPa shows a short first and second stage then a long tertiary stage. The second stage last 9 h and the strain rate is basically stable. After 12 h from the beginning of creep, the strain rate increased rapidly. The specimen is broken when the creep time up to 40.5 h.

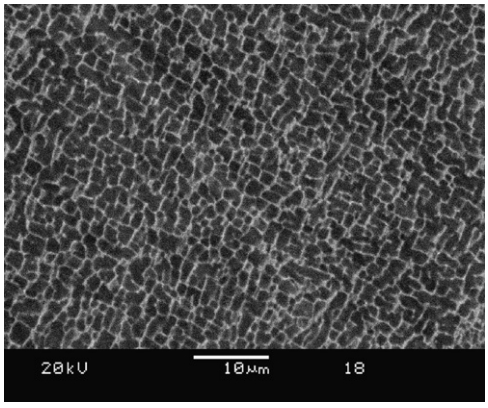

Fig. 3 Microstructure of IC6SX alloy after heat treatment (1300 °C/10 h+870 °C/32 h).

3.2. *Microstructure of the alloy before and after creep*

The microstructures of the as-cast alloy are shown in Fig. 2, showing the typical as-cast dendrite structure. The as-cast alloy is mainly composed of four phases: γ-Ni(Mo), γ′-Ni_3(Al,Mo), Y-NiMo, trace boride, and two types of γ′ phase exist in the alloy, i.e., eutectic γ′ and precipitated γ′ phase. The total amount of γ′ phase is about 75% in volume percent and the sizes of precipitated γ′ phases are 1–3 μm in dendrite arm area B and 0.1–0.5 μm in interdendritic area A, as shown in Fig. 2(b). The Y-NiMo phase enveloped by γ′ precipitate in interdendritic area formed by the reaction of γ-Ni(Mo)→Y-NiMo+γ′-Ni_3(Al,Mo).

The experimental results show that the proper homogenizing treatment of the present alloy was 1300 °C/10 h+870 °C/32 h. Fig. 3 shows the microstructure of the alloy before creep test. The microstructure consists of γ and γ′ phase, and the size of γ′ phase is about 1 μm. It can be seen that the large Y-NiMo phase and γ/γ′ eutectic entirely disappeared in the interdendritic regions after heat treatment.

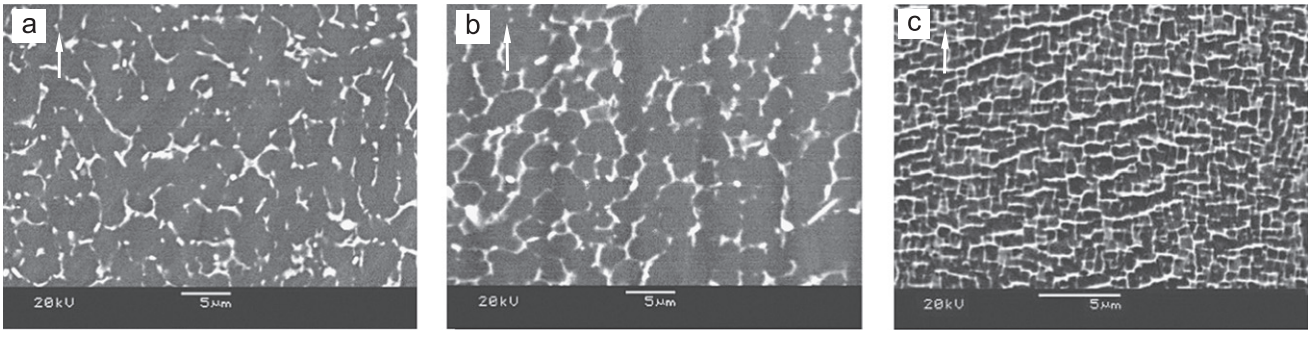

Fig. 4 Micrographs of the alloy after creep under different conditions for 100 h. (a) 760 °C/593 MPa; (b) 980 °C/205 MPa; (c) 1100 °C/75 MPa.

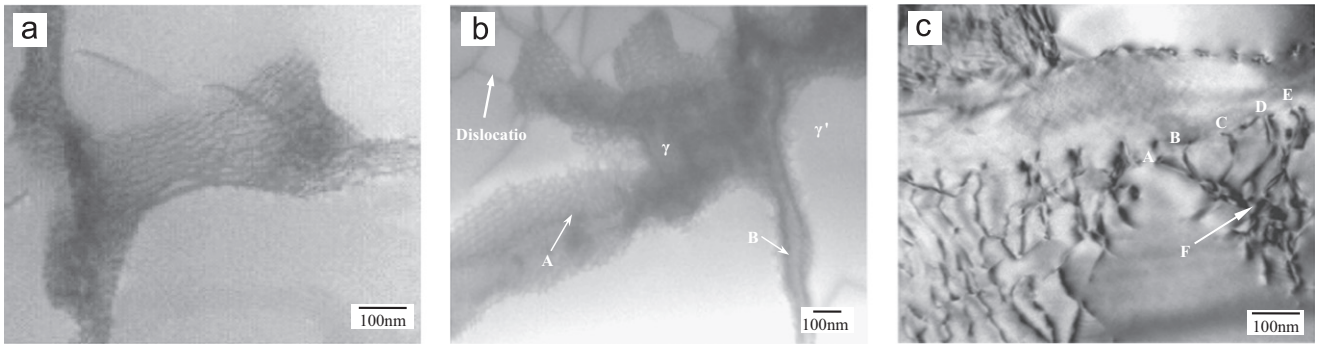

Fig. 5 TEM Micrographs of the alloy after creep under different conditions for 100 h. (a) 760 °C/593 MPa; (b) 980 °C/205 MPa; (c) 1100 °C/75 MPa.

Fig. 4 shows the change of microstructure of IC6SX alloy after being tested under the conditions of 760 °C/593 MPa, 980 °C/205 MPa and 1100 °C/75 MPa for 100 h. It can be seen that the directional coarsening of γ′ phase under 760 °C/593 MPa is most obvious, which belongs to Parallel–Normal coarsening type [15]. No rafted structure was observed for the specimens under 760 °C/593 MPa, 980 °C/205 MPa, and the rafted γ′ phase was only observed in the specimen under 1100 °C/75 MPa. During creep, the cubic γ′ phase is transformed into the rafted structure. Usually, the kinetics of the γ′ coarsening depends on the thermodynamic driving force. Because the specimens under 760 °C/593 MPa, 980 °C/205 MPa have higher shear stresses, which can make the smaller γ′ phases dissolve and the larger ones grow, and the kinetics are generally controlled by volume diffusion in which the solute is transferred through the matrix from the shrinking particles to the growing ones [16].

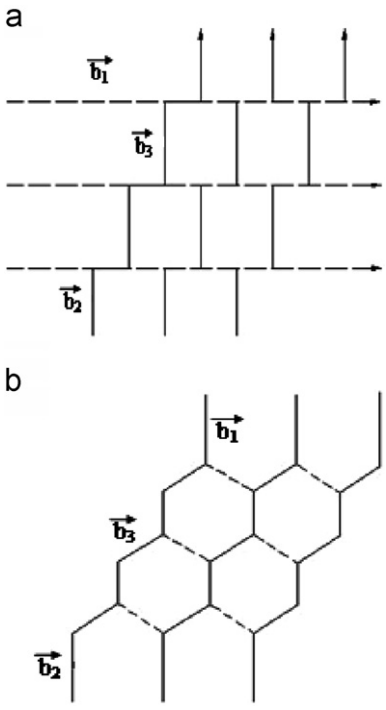

Fig. 6 Schematic diagram of dislocation network formation in the single crystal alloy [14].

3.3. *Observation of dislocation configuration of the crept specimens*

Fig. 5 shows the TEM microstructure of the specimens after creep for 100 h. It can be seen from Fig. 5(a), a large number of dislocations generated in the γ channels under 760 °C/593 MPa. The dislocation in one matrix channel moves into the other matrix channels subjected to compression stress by means of cross-slip [17,18].

It can be seen from Fig. 5(b) that in the specimens tested under the condition of 980 °C/205 MPa, dislocation is activated and multiplied by dislocation reactions along the horizontal channels (shown in the arrow A). High-density dislocation networks are generated in the γ channels. The schematic diagram of dislocation networks are shown in Fig. 6 [16], dislocations of b_1 and b_2, with different Burgers vector, meet and generate a new dislocation b_3.

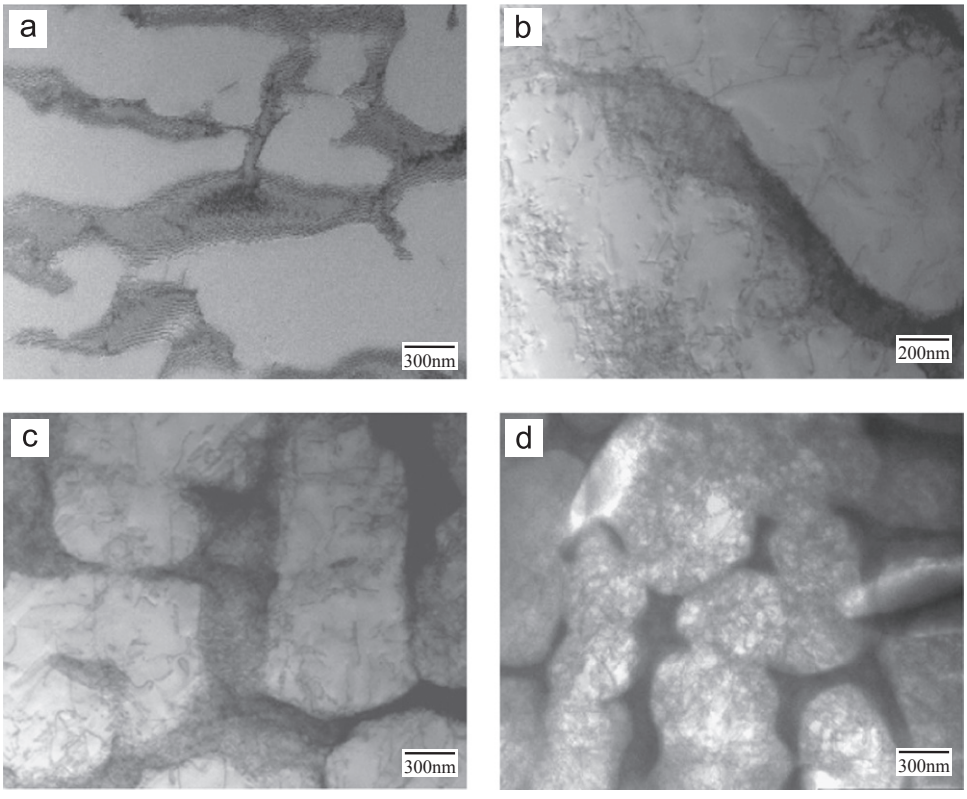

Fig. 7 Dislocation configuration of the alloy in different creep stages under 1070 °C/137 MPa. (a) Primary stages; (b) steady stages; (c) accelerating stages; (d) after failure.

The formation of dislocation networks provides an ideal structure for creep resistance because the mobile dislocations will be hindered by other dislocations which slipped on the different orientations.

At the same time, the dislocations are observed at the γ/γ′ interface in the longitudinal channel (shown in the arrow B) and dislocation networks are not observed. The reasons of this phenomenon is that the vertical tensile stress acts on the horizontal channel, which enables it expansion and wider to both sides. Contrary to the horizontal channel, longitudinal channel is squeezed and the width is narrow [19,20]. In the horizontal channels, the dislocations pile up and result in stress concentration. When the stress concentration reaches a certain level, movement dislocations cut into the γ′ phases and result in the decrease of creep properties. The results above indicate that the dislocation in one matrix channel can not only moves into the other matrix channels subjected to compression stress by means of cross-slip, but also cut through the γ′ particles under the creep test condition of 980 °C/205 MPa for 100 h.

It can be seen from Fig. 5(c) that the dislocation walls and dislocation tangles were formed at the interface of γ′/γ by large amounts of dislocation glide. For example, the dislocations A,B,C, D and E cut into the γ′ matrix, and meet in F region (shown by the arrow). Because of the low stress is not enough to drive dislocations continuously, the dislocation walls and dislocation tangles exist mainly at the interface of γ′/γ.

Fig. 7 shows dislocation configuration of the alloy in different creep stages under 1070 °C/137 MPa. It can be seen from Fig. 7(a) that dislocations moved in the γ channel in the first stage, and the motion of dislocations were prevented by the γ′ matrix. The formation of fine and continuous γ′ phase provides an ideal structure for creep resistance because the mobile dislocations will be hindered from passing these γ′ phase. When the creep time up to the second stage, the density of dislocations in the γ channels increases and dislocations block each other, as shown in Fig. 7(b). APB (anti-phase boundary) can be observed in the γ′ phases. The formation of APB can be attributed to the high stress. Although the test was carried out at constant load, the true stress increased rapidly during the creep. The increasing of stress makes dislocations cut into the γ′ particles and APB formed easily.

Fig. 7(c) shows the microstructure of the tertiary stage of the creep specimen. It can be seen that, in the stage, the dislocation multiplication occurred when dislocations with different Burgers vector meet and react. With the increasing of dislocations in the γ′ matrix, the invigoration effect of γ′ matrix are reduced and the strain rate increase rapidly resulting in fracture. Fig. 7(d) shows the microstructure of specimen after failure. It can be seen that a lot of dislocations cut into the γ′ particles and the rafted γ′ phase has been damaged.

4. Conclusions

1) An investigation on the creep behavior and microstructure of Ni_3Al base IC6SX alloy with [001] orientation during creep deformation under 760 °C/593 MPa, 980 °C/205 MPa and 1100 °C/75 MPa was conducted. For the test conditions of 760 °C/593 MPa and 980 °C/205 MPa, the first and second stages of creep process are short and the creep strain can reach to about 0.6%–0.7%. However, the creep curve of the alloy under 1100 °C/75 MPa has no third stage and the strain rate is about 0.35%. The results indicate that the alloy there is good creep properties at elevated temperature.
2) TEM observations indicate that the dislocation configuration and movement pattern are different under the different test conditions. The dislocation moves in γ channel by means of cross-slip under 760 °C/593 MPa. The dislocation in one matrix channel can not only moves into the other matrix channels by means of cross-slip, but also cut into the γ′ particles under 980 °C/205 MPa for 100 h. The dislocation walls and dislocation tangles exist mainly at the interface of γ′/γ under 1100 °C/75 MPa. The test results under 1070 °C/137 Mpa show that dislocation move in the γ channel in the primary stage, and cut into the γ′ phase from the γ/γ′ interface in the secondary stage. In the tertiary creep stage, dislocation pileup is observed in the γ channel and γ′ phase, and dislocation multiplication occurred.

Acknowledgments

The authors would like to express their appreciation and gratitude to the National Natural Science Foundation of China (No. 50971005) and Chinese Universities Scientific Fund (No. 2013RC0402), which provided support, and the reviewers for their advice, comments and unfailing encouragement.

References

[1] J.C. Zhao, J.H. Westbrook, Ultrahigh-temperature materials for jet engines, MRS Bulletin 28 (9) (2003) 622–627.
[2] S.Y. Qu, Y.F. Han, L.G. Song, Effects of alloying elements on phase stability in Nb–Si system intermetallics materials, Intermetallics 15 (5–6) (2007) 810–813.
[3] S.G. Tian, X.F. Yu, J.H. Yang, et al., Deformation features of a nickel-base superalloy single crystal during compression creep, Materials Science and Engineering A 379 (2004) 141–147.
[4] K. Chen, L.R. Zhao, J.S. Tse, Atomic mechanism of the Re and Ru strengthening effect on the γ–γ′ interface of Ni-based single-crystal superalloys: a first-principles study, Philosophical Magazine 83 (14) (2003) 1685–1698.
[5] W.D. Pridemore, Stress-rupture characterization in nickel-based superalloy gas turbine engine components, Journal of Failure Analysis and Prevention 8 (3) (2008) 281–288.
[6] L.J. Carroll, Q. Feng, J.F. Mansfield, et al., Elemental partitioning in Ru-containing nickel-base single crystal superalloys, Materials Science and Engineering A 457 (1–2) (2007) 292–299.
[7] Y.F. Han, S.H. Li, Y. Jin., et al., Effect of 900–1150 °C aging on the microstructure and mechanical properties of a DS casting Ni_3Al-base alloy IC6, Materials Science and Engineering 193 (1995) 899–905.
[8] Y.F. Han, S.H. Li, M.C. Chaturvedi, Microstructural stability of the directionally solidified γ prime-base superalloy IC6, Materials Science and Engineering 160 (1993) 271–276.
[9] Y.F. Han, C.B. Xiao, Effect of yttrium on microstructure and properties of Ni_3Al base alloy IC6, Intermetallics 8 (6) (2000) 687–691.
[10] Y. Cheng, H. Zhang, L.W. Song, et al., Effect of Re element on oxidation resistance of Ni_3Al–Mo based alloys at 1150 °C, Transactions of Nonferrous Metals Society of China 22 (3) (2012) 510–515.
[11] K.B. Povarova, N.K. Kazanskaya, A.A. Drozdov, et al., Influence of rare-earth metals on the high-temperature strength of Ni_3Al-based alloys, Russian Metallurgy (Metally) 2011 (1) (2011) 47–54.
[12] L.W. Jiang, S.S. Li, M.L. Wu, et al., Effect of dendrite arm spacing and the γ′ phase size on stress rupture properties of Ni_3Al-base single crystal superalloy IC6SX, Science China Technological Sciences 53 (6) (2010) 1460–1465.

[13] H.L. Goldenstein, Y.R. Silva, Y.S. Nunes, et al., Designing a new family of high temperature wear resistant alloys based on Ni_3Al IC: experimental results and thermodynamic modeling, Intermetallics 12 (7) (2004) 963–968.
[14] K.J. Hemker, M.J. Mills, W.D. Nix, Investigation of the mechanisms that control intermediate temperature creep of Ni_3Al, Acta Metallurgica et Materialia 39 (8) (1991) 1901–1913.
[15] A. Fredholm, J.L. Strudel, On the creep resistance of some nickel-base single crystals, Superalloys, AIME, Warrendale, PA211–220.
[16] L.R. Liu, T. Jin, N.R. Zhao, et al., Creep deformation mechanism in a Ni base single crystal superalloy, Acta Metallrugica Sinica 41 (11) (2005) 1215–1220.
[17] S.G. Tian, H.H. Zhou, J.H. Zhang, et al., Aspects of primary creep of a single crystal nickel-base superalloy, Materials Science and Engineering 262 (1999) 271–278.
[18] A. Dlouhy, On the formation and motion of $<010>$ dislocation during high temperature low stress creep of superalloy single crystals, Materials Science and Engineering A 234 (8) (1997) 958–961.
[19] W. Duncan, L.W. MacLachlan, Constitutive modelling of anisotropic creep deformation in single crystal blade alloys SRR99 and CMSX-4, International Journal of Plasticity 17 (4) (2001) 441–467.
[20] J.R. Li, K.G. Wang, Y.S. Luo, et al., Creep behavior of single crystal superalloy DD6 at 760 °C and 980 °C, Materials Science Forum 539 (3) (2007) 3118–3123.